Application Note 24. Analysis of electrochemical fluctuations for fast impedance spectroscopy

Serge Kernbach

***Abstract*—The application note 24 (AN24) is devoted to statistical and spectral description of ionic dynamics based electrochemical fluctuations. These two approaches allow characterizing weak electrochemical markers and ionic properties of liquid and organic samples in reliable and reproducible way. The statistical and spectral modules are enabled in EIS, biosensor and phytosensor applications, they are implemented as a post-processing of measured data, performed in real time. New implementation of the signal scope mode offers an express analysis with the measurement time of 4.4 ms, known as fast EIS, and can underlie real-time interfacing technology in biohybrid systems, interactions with organic tissues on ionic level. AN24 explains the main methodological and technical aspects, settings and provides examples of measurements and obtained results. Calibration and five different measurement strategies are discussed and illustrated with examples.**

firmware version: > 1189.41; client version: > 1.3.92
original preparation: October, 2018; revisions: 2022, 2024

I. Introduction

The AN24[1] considers fluidic, biosensing, phytosensing and biohybrid applications, where weak ionic changes of aqueous solutions, colloidal or organic samples should be detected, measured and characterized.

Ionic dynamics has a molecular character and reflects multiple chemical and physical processes – changes in number and mobility of ionic groups, building of ionic products in chemical reactions (especially with gases), biological processes or dynamics of electrochemical systems. Applying electric field and additional optical or magnetic excitations during measurements involve different physical processes up the nuclear level of spin isomers. Processes that produce such ionic changes are denoted further as *non-chemical treatment* of corresponding samples – to emphasize their underlying physical mechanisms.

Electrochemical impedance spectroscopy (EIS) delivers data about ionic properties and ionic dynamics, and excites samples by the potential V_V^f, electrical current between electrodes is measured as a signal V_I^f. Both V_V^f and V_I^f are recorded, the relationship between them reflects the ionic content and mobility of ions at frequency f [1], [2]. There are five different ways how the EIS data can be handled and interpreted. This includes not only the measurement but also the preparation of samples and experimental methodology.

1) The excitation V_V^f and response V_I^f signals allow calculating two main parameters with frequency response analysis (FRA) – the magnitude $M(f)$ and phase $P(f)$ of impedance, as well as several additional values such as the correlation between V_V^f and V_I^f, the Nyquist Plot and others. This enables mapping measured data to electrochemical models, for instance, to identify specific dissolved substances based on their RC models.

2) Since different ions are continuously produced in water (e.g. by dissolving gases, self-ionization or proton-hopping mechanisms), EIS data are sensitive to the history of samples – in which conditions samples are prepared and stored. This includes light, temperature, EM fields, mechanical distortions, several other factors. By comparing two samples that are prepared in similar conditions (where all environmental influences between control and experimental samples differs in one factor), it is possible to identify whether the experimental sample was exposed by this factor before the measurement. This approach underlies the double differential methodology [3], and allows characterizing exposed fluid in regard to unexposed fluid. This methodology is denoted as *Measurement-after-Treatment (MaT)*.

3) The dynamics of EIS parameters can be of interest, where excitation $V_V^{f,t}$ and response $V_I^{f,t}$ signals depend not only on the frequency f but also on time t [4] (non-stationary EIS systems). Since the created by EIS electric field interacts with self-ionization process (this involves several quantum effects [5]), the continuous EIS is sensitive to micro- (e.g. quantum) and macro- factors applied to samples during the measurements and allows observing them on a macroscopic scale as a change of impedance in real time. This methodology is denoted as *Treatment-during-Measurement (TdM)*. Since TdM produces less disturbances than MaT, the TdM strategy is mostly utilized for measuring weak ionic effects and is used in biohybrid interfaces.

4) Samples during EIS measurements can be additionally excited by optical, magnetic or other means. This approach is denoted as excitation spectroscopy and is implemented in the hardware of CYBRES EIS systems. The excitation spectroscopy allows characterizing the *dynamical excitation-response properties* of fluidic electrochemistry (see Sec. X).

5) Electrochemical fluctuations in V_I^t can be analyzed from the viewpoint of statistical/spectral properties. Here, the excitation signal V_V^t has either a harmonic (sinusoidal) or nonharmonic (random) form. In both cases the noise in V_I^t is extracted and analyzed, e.g. with discrete Fourier transformation (DFT). This approach is known as fast EIS [6] and has two different aspects: 1) long-term changes of electrochemical stability and 2) short-term fluctuations of current and potential, see Fig. 1.

This application note primarily focuses on the last approach. The statistical analysis of electrochemical noise is well-known

CYBRES GmbH, Research Center of Advanced Robotics and Environmental Science, Melunerstr. 40, 70569 Stuttgart, Germany, Contact author: serge.kernbach@cybertronica.de.com

[1] See video https://www.youtube.com/watch?v=K66RQ4ZfGho for AN24.

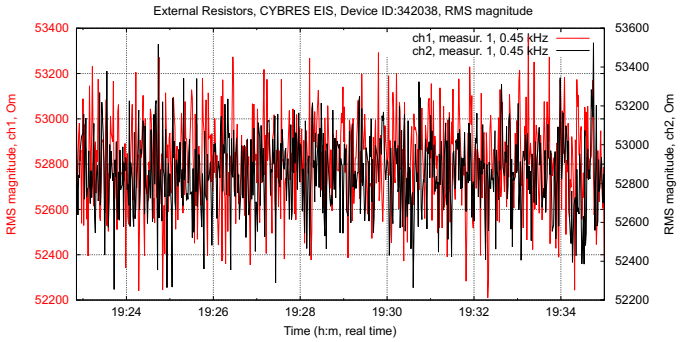

(a)

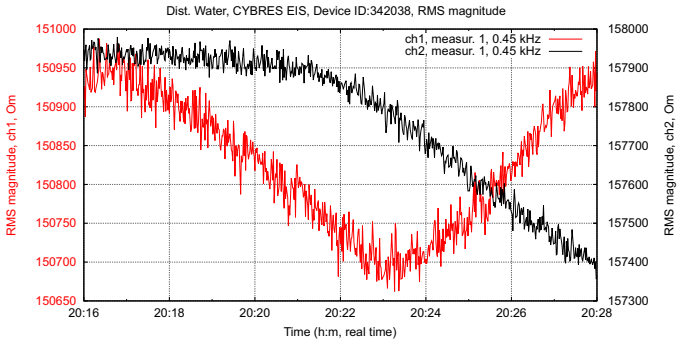

(b)

Fig. 1. Different time dynamics of noisy signals. **(a)** Short-term noise (two external resistors); **(b)** Long-term electrochemical stability (two containers with water, one water sample is non-chemically processed). Different temporal dynamics of both fluids (that represents an electrochemical stability) and different parameters of current fluctuations in both channels are observed.

[7], [8] in the corrosion monitoring, surface properties analysis, tests of dynamical behaviour (e.g. gas bubble formation). The statistical analysis is used in all applications of MU systems and is related to the values of 'RMS magnitude' $M^{RMS}(t)$, 'FRA phase' $P^C(t)$, the 'correlation' $C(t)$ as well as the input potentials dV (in bio-/phyto- sensing and in 4-electrode EIS), calculated at time steps t.

II. Understanding the Origin of Electrochemical Noise in EIS

The functional scheme of generating the V_V and V_I signals in EIS systems is shown in Fig. 2. Waveform generation is performed in digital way by using DAC and the following functions

$$V_V^{exc}(n) = A\sin(\frac{\pi}{k}n), \quad n = 0...N_{DAC}, \tag{1}$$

$$V_V^{exc}(n) = rand(), \quad n = 0...N_{DAC} \tag{2}$$

where A, k are coefficients, N_{DAC} is the number of samples, $rand()$ is a generator of pseudorandom numbers with properties of white noise. The expression (1) is used for EIS with FRA analysis, the expression (2) is used for fast EIS and with DFT and wavelet analysis, see Sec. IV. The signal $V_V^{exc}(n)$ is stored in V_{DAC} array with max 4000 points.

The excitation $V_V^{exc}(n)$ and response $V_I^{exc}(n)$ signals are sampled by synchronous 1.1 mps ADCs and stored in memory as $V_V^f(n)$ and $V_I^f(n)$ arrays. Hardware implementation

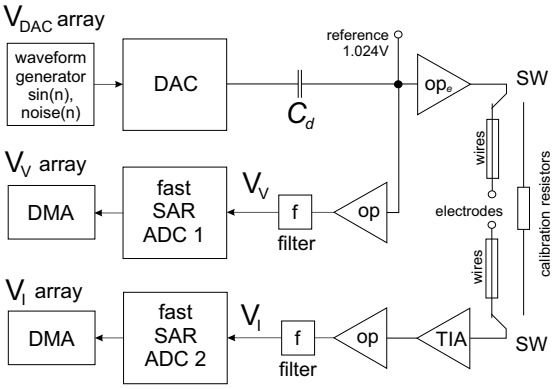

Fig. 2. Functional scheme of generating the V_V and V_I signals in the EIS systems, ADC/DAC – analog-to-digital and digital–to-analog converters, OP – operational amplifier, TIA – transimpedance amplifier with programmable gain (50x, 500x, 5000x, 50000x), DMA – direct memory access, SW – multiplexers (electronic switch). Both 1.1 mps SAR ADCs are synchronously sampling.

ensures a sampling of full period of sinusoidal signal and produces 4x2048 sampled values of two-channel $V_V^f(n)$ and $V_I^f(n)$ signals for further analysis. ADC has three predefined sample rates Δt =(1.125 μs, 4.275μs, 53.1μs) per sample, and always produces $N_{ADC} = 2048$ samples per channels, i.e. durations of measurement $T = \Delta t N_{ADC}$ for all three ranges are T =(2.304ms, 8.7552ms, 108.7488ms), see Table I.

TABLE I
Parameters of sampling, main clock 80MHz, each ADC conversion requires 18 CPU cycles, $N_{ADC} = 2048$ samples per channels, $\Delta f = 1/T$ and $f_{max} = 1024\Delta f$, k – the correction coefficient between DAC- and ADC-based f_{max} sampling parameters.

range	divider	Δt, μs	T, ms	Δf, Hz	f_{max}, kHz	k
based on ADC sampling only						
1	4	1.125	2.3	434,02	444.(4)	
2	18	4.275	8.75	114,21	116.95	
3	235	53.1	108.74	9,19	9.4	
based on DAC for harmonic signals, see Sec. IV						
1		1.085	2.(2)	450	460.8	0.9645
2		4.882	10	100	102.4	1.142
3		61.035	125	8	8.192	1.1474

Due to a full-period sampling, the number of samples N_{DAC} in (1) is not related to N_{ADC} in $V_V^f(n)$ and $V_I^f(n)$. Increasing N_{DAC} leads to a higher sampling rate of DAC (more points for the same waveform), whereas the sampling rate of ADC remains the same. Thus, in case of FRA for harmonic signals, we select $N_{DAC} = N_{ADC}$. However, selection of N_{DAC} has consequences for analyzing spectral properties of electrochemical fluctuations, especially for the expression (2). Generally, DFT depends on the sampling rate of ADC, see Sec. IV, but it is sensitive to selection of N_{DAC}. If ADC samples faster than DAC produces the next sample, that is equivalent to

$$N_{ADC} > N_{DAC} \tag{3}$$

it will reduce the maximal analysing frequency of (2) and spectral properties of electrochemical fluctuations become defined

by DAC. If

$$N_{ADC} < N_{DAC} \tag{4}$$

ADC will be not able to capture all samples generated by DAC, but fluidic/organic samples are exited by higher frequency of random signal.

Considering the scheme in Fig. 2, we see that fluctuations have three components:

1) electronic noise from operational amplifiers, DAC/ADC that is similar in both $V_V^f(n)$, $V_I^f(n)$;
2) electromagnetic interference (EMI in wires);
3) electrochemical fluctuations in $V_I^f(n)$.

Since the external path between OP_e and TIA represents the current loop with shielded wires, EMI part of noise has a neglectably small amplitude. The difference between electronic noise in $V_V^f(n)$ and electrochemical noise in $V_I^f(n)$ is well visible in Figs. 3 and 4. Generally, electronic noise and EMI represent artifacts that cannot be fully removed from the analysis. Electrochemical fluctuations appear at both waveforms (1) and (2), the main difference lies in their character: harmonic signals (1) produce fluctuations from one frequency f, where as the white broadband noise (2) produces fluctuations from many different frequencies (in the manner of fast EIS).

Electronic and electrochemical fluctuations have different impact on the EIS system. The differential EIS uses a phase-amplitude detection of excitation and response signals. The RMS values $V_V^{RMS}(f)$ and $V_I^{RMS}(f)$ are calculated as

$$V_I^{RMS}(f) = \sqrt{\sum_{n=0}^{N-1} \frac{1}{N} \left(V_I^f(n)\right)^2}, \tag{5}$$

$$V_V^{RMS}(f) = \sqrt{\sum_{n=0}^{N-1} \frac{1}{N} \left(V_V^f(n)\right)^2}. \tag{6}$$

They are used for calculating so-called 'RMS resistivity'

$$M^{RMS}(f) = \frac{V_V^{RMS}(f)}{V_I^{RMS}(f)}. \tag{7}$$

$M^{RMS}(f)$, calculated from RMS values, corresponds to the magnitude of impedance $M(f)$, calculated by frequency-response-analysis (FRA) [1]. The $V_I^f(n)$, $V_V^f(n)$ samples allow calculating two other values – the correlation $C(f)$ and phase $P^C(f)$ (based on the lock-in phase detector for harmonic signals)

$$C(f) = \frac{1}{N} \sum_{k=0}^{N-1} V_I^f(n) V_V^f(n), \tag{8}$$

$$P^C(f) = \frac{180}{\pi} \cos^{-1}(\gamma(f) C(f)), \tag{9}$$

where $\gamma(f)$ is a f-dependent amplitude-based coefficient, detected in V_I, V_V signals. The RMS-based calculation has several advantages over FRA methods [2], and thus is used in EIS systems.

The values of $V_V^f(n)$, $V_I^f(n)$ and $M^{RMS}(f)$, $C(f)$, $P^C(f)$ represent different time scales and react on noise in different ways. The $V_V^f(n)$, $V_I^f(n)$ signals are accessible in the 'signal scope' mode with about 4.6 ms for a single differential measurement. The $M^{RMS}(f)$, $C(f)$, $P^C(f)$ signals are accessible in the 'continuous measurement' mode with about 600 ms for a single differential sampling. To some extent, the dynamics of (7), (8), (9) reproduces a long-term behavior of the 'signal scope' mode.

As shown in Fig. 4, **the non-chemical treatment changes not only the amplitude of sinusoidal response signal** $V_I^f(n)$, and thus the values of $M^{RMS}(f)$, $C(f)$, $P^C(f)$ used in continuous mode analysis, **but also the electrochemical noise of this signal**.

The amplitude-based changes are covered by the 'continuous mode' methodology with regression analysis and corresponding statistical methods, see the Application notes 26 and 27 [9], [10]. For noise-based analysis, the three following methods are utilized:

1) Analysis based on statistical moments applied to $M^{RMS}(f)$ in 'continuous mode'. Since the expression (7) contains both $V_V^{RMS}(f)$ and $V_I^{RMS}(f)$, the electrochemical noise is 'amplified' by electronic noise. This method can be used for e.g. assessment of long-term electrochemical stability.

2) Analysis based on statistical moments applied to $V_I^f(n)$ in 'signal scope mode'.

3) Analysis of spectral properties of $V_I^f(n)$, based on discrete Fourier transformation (DFT).

The following sections describe these methods in more detail.

III. Extracting electrochemical noise

As mentioned in the previous section, $V_V^f(n)$ contains only electronic noise, whereas $V_I^f(n)$ has a combination of electronic and electrochemical noise. Thus, before using statistical or spectral descriptors, the electrochemical noise should be extracted from sinusoidal $V_I^f(n)$.

1) As the simplest approach, $V_I^f(n)$ can be directly analysed.

2) Possible alternative is to analyse the channel-differential signal $\Delta_{ch}^f(n)$

$$\Delta_{ch}^f(n) = V_{ch1}^f(n) - V_{ch2}^f(n). \tag{10}$$

applied to both $V_V^f(n)$ and $V_I^f(n)$. Fig. 5 demonstrates an example of this approach. We observe zero biased signal for $V_V^f(n)$, but still sinusoidal signal for $V_I^f(n)$ due to small electrochemical differences of both fluids. Thus, the channel-different methods is not suitable for analysing electrochemical noise in one of channels.

3) To remove periodical components from sinusoidal signals, the time-delayed values can be calculated only from $V_I^f(n)$

$$\Delta_t^f(n) = V_I^f(n) - V_I^f(n-1) \tag{11}$$

so that the function (1) is transformed with sin^{-1} to the constant $\frac{\pi}{k}$ with the following transformation:

$$V_I^{exc}(n) - V_I^{exc}(n-1) \rightarrow$$
$$\left| sin^{-1}\left(\frac{V_I^f(n)}{A}\right) - sin^{-1}\left(\frac{V_I^f(n-1)}{A}\right) \right| =$$
$$= \frac{\pi}{k} n - \frac{\pi}{k}(n-1) = \frac{\pi}{k}, \quad n = 0...N, \tag{12}$$

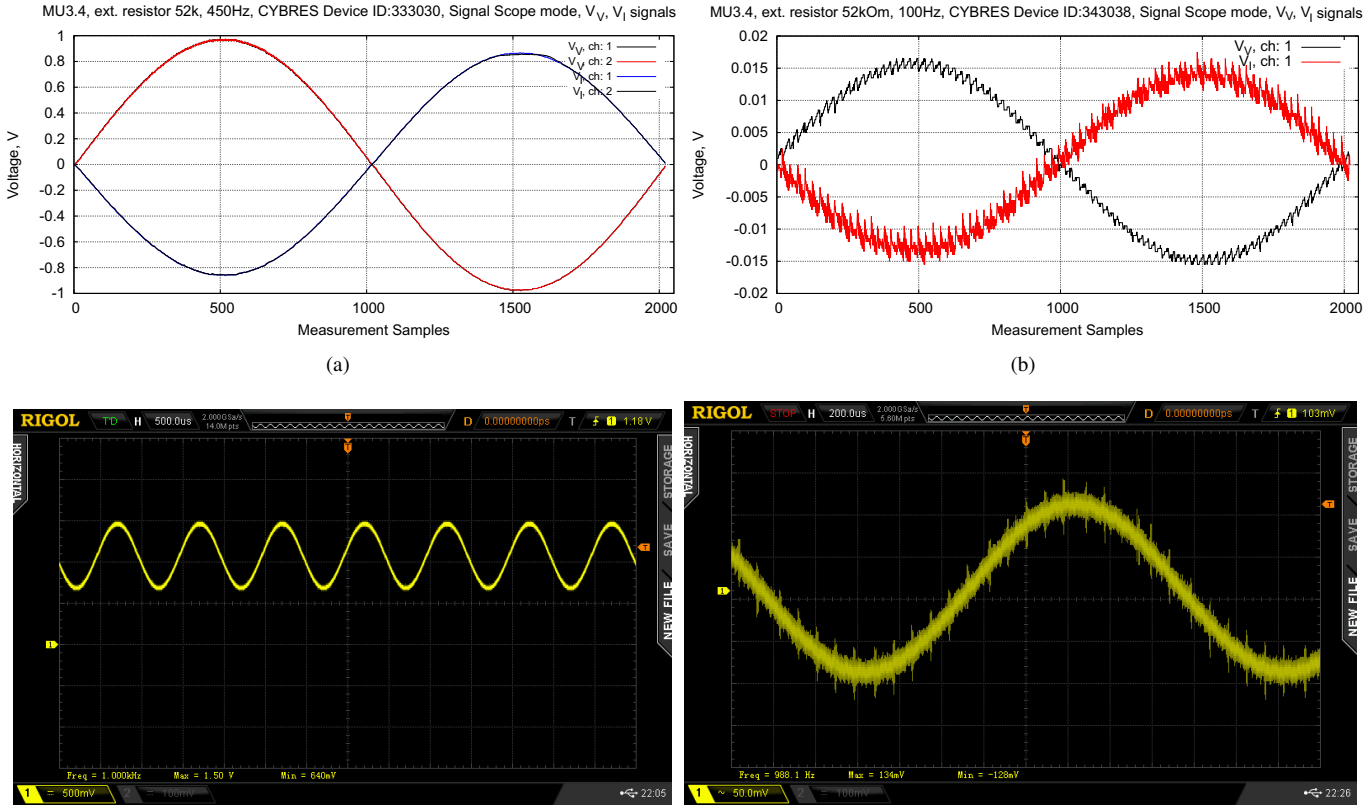

Fig. 3. **(a,b)** Signal scope mode with two excitation and two response signals (ch1 and ch2) with high ($\pm 1V$) and middle ($\pm 0.1V$) excitation ranges; **(c,d)** Excitation signals measured on electrodes of the channel 1 in both cases.

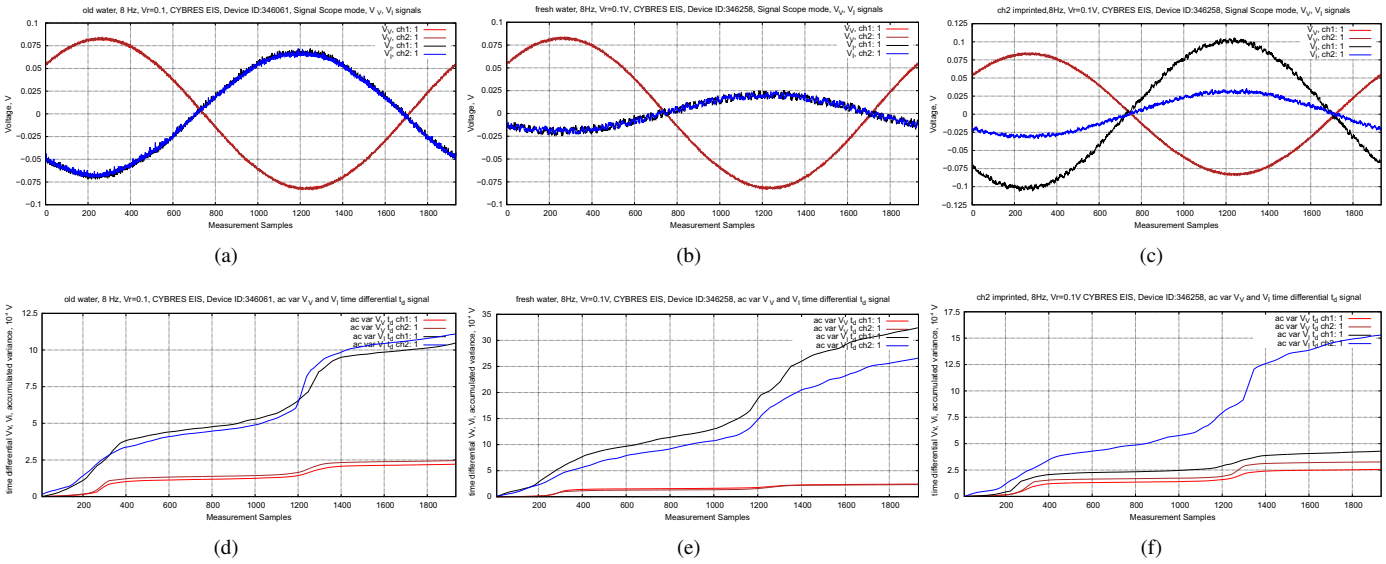

Fig. 4. Examples of different electrochemical noise in signal scope mode (lower row, accumulated variance is shown) of equal fluids with different non-chemical treatment history (upper row), the middle excitation range $\pm 0.1V$ and excitation frequency 8 Hz are used; **(a,d)** 'Fresh-filled' distilled water with initial conductivity about 2 $\mu S/cm$; **(b,e)** 'Old-filled' distilled water with initial conductivity about 2 $\mu S/cm$, the fluids are stored in closed measurement containers with frequently performed measurements; **(c,f)** The same original distilled water as in previous cases, but the fluidic sample in channel 2 is non-chemically treated.

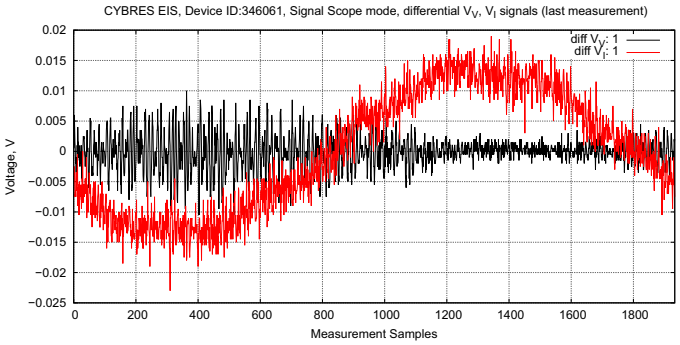

Fig. 5. The channel-differential noise in $V_V^f(n)$ and $V_I^f(n)$ signals (the high excitation range $\pm 1V$, 8 Hz). The sinusoidal components in $V_I^f(n)$ are still present.

The coefficient A reflects hardware-related changes in amplitudes and should satisfy

$$A \geq V_I^f(n), \quad n = 0...N \tag{13}$$

for the maximal amplitude of $V_I^f(n)$. The value $\frac{\pi}{k}$ is a constant from the viewpoint of (1), however it contains high-amplitude inhomogeneous noise, see Fig. 6. Two peaks in these graph arise because of DAC, that produces 'upper' and 'bottom' parts of sinusoidal signal with a low number of digits – this changes the noise-to-signal ratio across the sinusoidal curve. Since the noise is always amplitude-dependent, the 'upper' part has a larger amplitude of noise than the lower part, see 7.

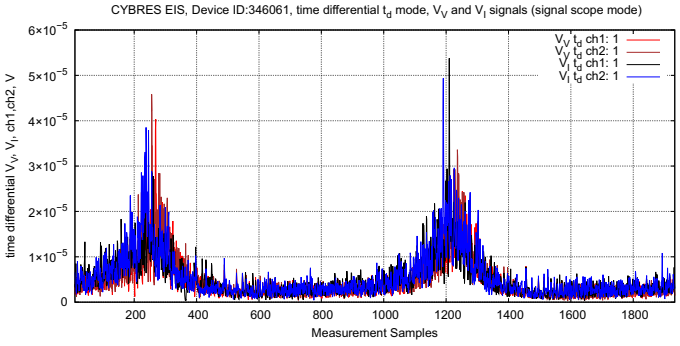

Fig. 6. The time-differential noise, the high excitation range $\pm 0.1V$, 8 Hz.

To demonstrate the difference between analysing directly $V_I^f(n)$ and the time-delayed $\Delta_t^f(n)$ signals, the Fig. 7 demonstrates the dynamics of standard deviation stDev (24) in both cases. We see that for $V_I^f(n)$, the amplitude of sinusoidal signal influences the amplitude of stDev, and electronic noise in $V_V^f(n)$ is larger than electronic+electochemical noise in $V_I^f(n)$. The case of $\Delta_t^f(n)$ produces a correct dependency between $V_V^f(n)$ and $V_I^f(n)$.

Generalizing this section, we conclude that the approach based on (1) is best suitable for extracting the electrochemical noise from one $V_I^f(n)$ channel. In the following, **this approach is denoted as 'time-delayed', applied to statistical moments and spectral Fourier analysis**. For comparison, the statistical moments can be applied directly to the $V_I^f(n)$ without time-delayed approach (12), denoted further as 'accumulated approach'. However, in this case, the variance (23) and all other metrices are impacted by the amplitude of sinusoidal signal.

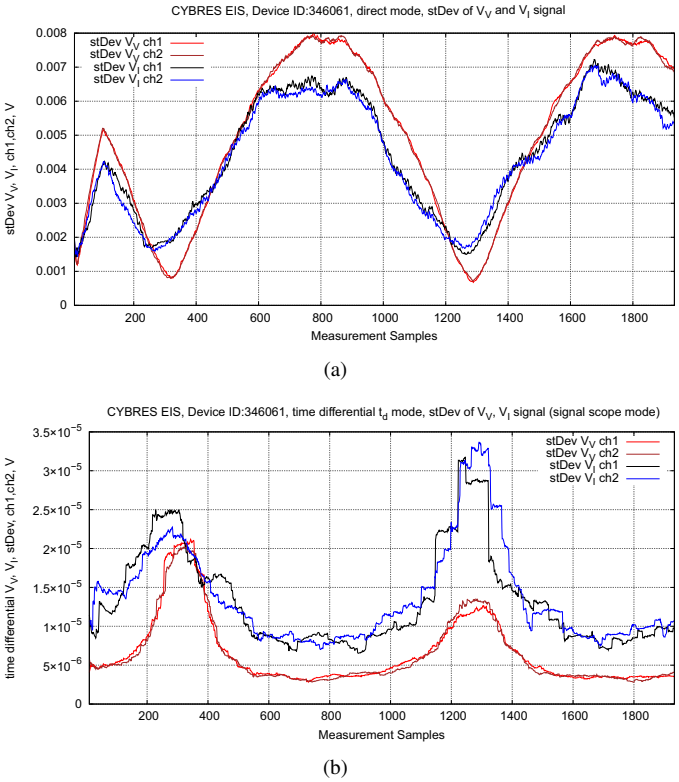

Fig. 7. Dynamics of standard deviation calculated **(a)** from $V_I^f(n)$ signal; **(b)** from $\Delta_t^f(n)$ signal obtained by (12). The moving window has 100 samples, the middle excitation range $\pm 0.1V$ at 8 Hz are used.

IV. Spectral Descriptors

To analyse spectral properties, $V_V^f(n)$, $V_I^f(n)$ arrays are processed by discrete Fourier transformation (DFT)

$$H_n = \sum_{k=0}^{M-1} V_k^f e^{-2\pi i k n/M} =$$

$$= \sum_{k=0}^{M-1} V_k^f [\cos(2\pi k n/M) - i \sin(2\pi k n/M)], \tag{14}$$

where M is the number of samples used for the transformation. Output data are plotted as magnitude $|H|$ and phase ϕ

$$|H| = \sqrt{Re(H)^2 + Im(H)^2}, \phi = \tan 2(Im(H), Re(H)). \tag{15}$$

The expression (14) is implemented directly as DFT as well as FFT with Danielson-Lanczos algorithm [11]. Despite a standard implementation, several aspect of this transformation should be taken into account.

1) Data in signal scope mode are sampled in such a way that $V^f(n)$ contains always full periods of sinusoidal signal produced by DAC. Sampling time Δt required for digitalizing one value of V^f can be calculated as

$$\Delta t = \frac{1}{f_{sampling}} / \frac{N}{P} = \frac{P}{N f_{sampling}}, \tag{16}$$

whereas $f_{sampling}$ is the sampling frequency produced by DAC, N is the length of V^f arrays, and P is the number of full periods in $V^f(n)$. Δf is the frequency step for a single sample H_n

$$\Delta f = \frac{1}{\Delta t M} = \frac{N f_{sampling}}{PM}. \quad (17)$$

For DFT with $N = M$

$$\Delta f = \frac{f_{sampling}}{P}, \quad (18)$$

the frequency scale of $|H_n|$ and ϕ_n (15) represents integer multiplicators of sampling frequency. The frequency scale ends up with N/2 samples, i.e. integer multiplicators are in the range [0...N/2] and the maximal frequency is

$$f_{max} = \frac{N f_{sampling}}{2P} \quad (19)$$

For instance, for $N = 2048$, $f_{sampling} = 450Hz, 100Hz, 8$ and $P = 1$ the maximal frequency is $f_{max} = 460.8kHz, 102.4kHz, 8.192kHz$.

DFT in the case $P = 2, 3, 4...$ and $P = 1$ produces slightly different results in relation to representation of noise ($P > 1$ decreases spatial resolution of a single period) and the maximum of $|H_n|$ (for $P = 1$ the maximum of $|H_n|$ is achieved at $n = 1$). The number of periods P is detected numerically for $f_{sampling} \leq 50kHz$, for all other frequencies the system is using estimation based on 50kHz signal.

If the excitation signal is not harmonic, f_{max} should be calculated based on ADC sampling, as shown in Table I. The main difference lies in Δt – in the case of harmonic signals generated by DAC, Δt is calculated based on a 'pure DAC frequency', which is important for Fourier transformation. In the case of non-harmonic signals, if the main excitation frequency is unknown, only sampling by ADC is considered for calculating Δt. Since hardware settings for frequency dividers in DAC and ADC are not related to each other (DAC has slightly lower frequency settings), this produces small differences for f_{max}. Selection of harmonic/non-harmonic is implemented in software (correction factors 1,0368000010368 0,8778396913844835 0,8714893617021277 for each ranges).

2) FFT imposes limitations on the value of M, e.g. the Danielson-Lanczos algorithm requires M to be an integer power of 2. To satisfy this requirement, M is set to 2^{11} that represents the maximal length of each channel of $V_V^f(n)$, $V_I^f(n)$ arrays handled by DMA, see Fig. 2. This condition (the length of V^f arrays is not equal to the number of samples used for FFT)

$$M > N, \quad (20)$$

has several consequences. First of all, increasing the size of V^f arrays by filling $M - N$ values with zeros (or applying windowing function) introduces nonlinearity and distortions, as shown in Fig. 8. Amplitude of distortions is substantially larger than the amplitude of noise. Secondly, the N/M factor shifts the frequency scale of (15) regarding the sampling frequency $f_{sampling}$, see Fig. 8(a),(b). Thus, FFT is not used for spectral descriptors, despite it has more efficient implementation than DFT.

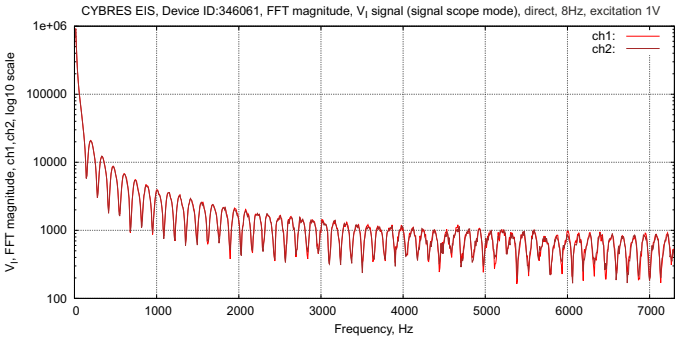

(a)

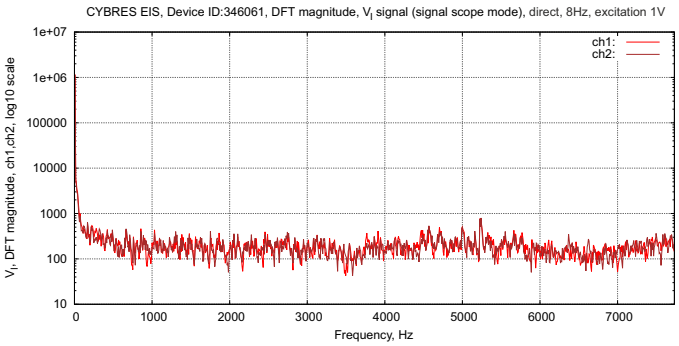

(b)

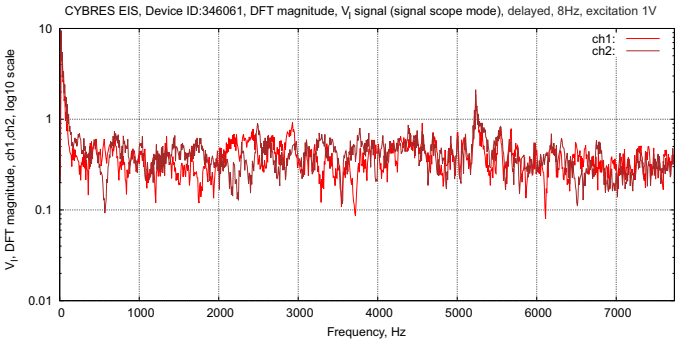

(c)

Fig. 8. Examples for magnitude of Fourier spectra calculated by **(a)** FFT with Danielson-Lanczos algorithm [11]; **(b)** DFT (14) applied directly to $V_I^f(n)$ array; **(c)** DFT (14) applied to time-delayed signal (12).

3) DFT (14) applied directly to $V_I^f(n)$ array and to time-delayed signal (12) is shown in Figs. 8(b),(c). As expected, the time-delay approach reduces the amplitude of first Δf and produces more linear spectrum.

4) For time-continuous estimators, calculated continually at time moments t, the following H_t value

$$H_t = \frac{1}{M} \sum_{k=2}^{M-1} |H_k^t|, \quad (21)$$

excluding the first Δf (the main amplitude) can be used as the spectral descriptor of electrochemical noise calculated channel-wise.

V. Fast electrochemical impedance spectroscopy

Ideas represented in Secs. III and IV are based on harmonic signals, where waveforms from $V_V^f(n)$ defines the analysing frequency, the current response $V_I^f(n)$ and, finally, properties of DFT. For the analysis it is important to capture the full period of $V_V^f(n)$ signal that imposes specific requirements on signals from DAC and signal sampling by ADC. In case of random (nonharmonic) excitation signal, the analysing frequency is defined by sampling rate of ADC and there is no need to consider the full period requirements. We will receive a maximal resolution, if the noise signal from DAC also has $N_{DAC} = 2048$ samples, generated at the same frequency. Given these considerations, we obtain for $T = N\Delta t$ for all three ranges (T=2.304ms, 8.7552ms, 108.7488ms) that will end up in the resolution of DFT Δf=1/T as (Δf =434.027Hz, 114.217Hz, 9.1955Hz) and maximal frequency at $N_{ADC}/2 = 1024$ points (f_{max} =444.4kHz, 116.9kHz, 9.41kHz).

VI. Descriptors based on statistical moments

This approach involves the notion of statistical moments in the following way. First, the values x_1, x_2, x_3, ..., x_n from $M^{RMS}(t)$, $P^C(t)$, $C(t)$ or $V_V^f(n)$, $V_I^f(n)$ are stored in corresponding buffers as a moving window over the input data flow. It means that at each step of data sampling, the last input value is always represented as x_n, all remaining data are shifted, $x_n = x_{n-1}$, $x_{n-1} = x_{n-2}$,..., $x_2 = x_1$. The size N of all input buffers is defined by the parameters 'bufferSizeDataPipesEIS' (for continuous mode) and 'bufferSizeDataPipesEISsig' (for signal scope mode) in the init.ini.

The mean of the values x_1, x_2, x_3, ..., x_n in each buffer is calculated as

$$\mu = \frac{1}{N}\sum_{i=1}^{N} x_i. \tag{22}$$

The second statistical moment is the variance

$$Var(x_1, ...x_n) = \frac{1}{N-1}\sum_{j=1}^{N}(x_j - \mu)^2, \tag{23}$$

its square root represents the standard deviation

$$\sigma(x_1, ...x_n) = \sqrt{Var(x_1, ..., x_n)}. \tag{24}$$

The third moment is the skewness

$$Skew(x_1, ...x_n) = \frac{1}{N}\sum_{j=1}^{N}\left[\frac{(x_j - \mu)}{\sigma}\right]^3 + k_s, \tag{25}$$

and the fourth moment is the kurtosis

$$Kurt(x_1, ...x_n) = \frac{1}{N}\sum_{j=1}^{N}\left[\frac{(x_j - \mu)}{\sigma}\right]^4 + k_k. \tag{26}$$

Since the statistical analysis is performed in real time over continuously sampled data, the expressions (23)-(26) are calculated at each step when new data sample is stored in the input buffers. This creates a time sequence of $Var()$, $Skew()$, $Kurt()$ applied to magnitude, phase and correlation that can be collected in the vector $\overline{\Phi^{1,2}(t)}$:

$$\overline{\Phi^{1,2}(t)} = \begin{bmatrix} Var(M^{RMS}(t)) \\ Var(P^C(t)) \\ Var(C(t)) \\ Skew(M^{RMS}(t)) \\ Skew(P^C(t)) \\ Skew(C(t)) \\ Kurt(M^{RMS}(t)) \\ Kurt(P^C(t)) \\ Kurt(C(t)) \end{bmatrix}. \tag{27}$$

Upper indexes denote the channels: $\overline{\Phi^1(t)}$ represents the channel 1, $\overline{\Phi^2(t)}$ – the channel 2.

Since $\overline{\Phi(t)}$ possesses a temporal behaviour, it needs to represent its dynamics in a compact form. It is implemented by accumulating these values in the following way:

$$V(t) = \sum Var(t), \tag{28}$$

$$S(t) = \sum Skew(t), \tag{29}$$

$$K(t) = \sum Kurt(t). \tag{30}$$

Example of $Var(M^{RMS}(t))$ and $V(t) = \sum Var(t)$ are shown in Fig. 9.

The expressions (28-30) can be considered as definite integrals between t_1 and t_2 – begin and end of measurements (or

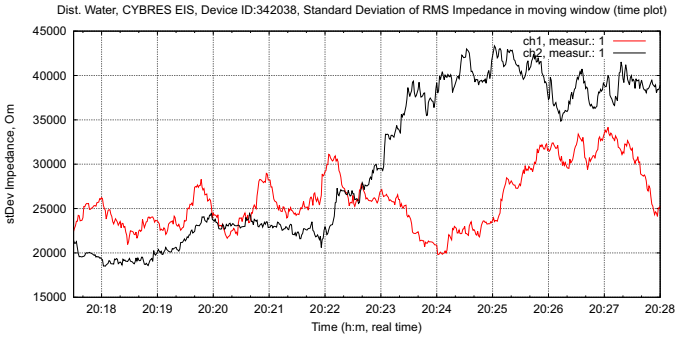

(a)

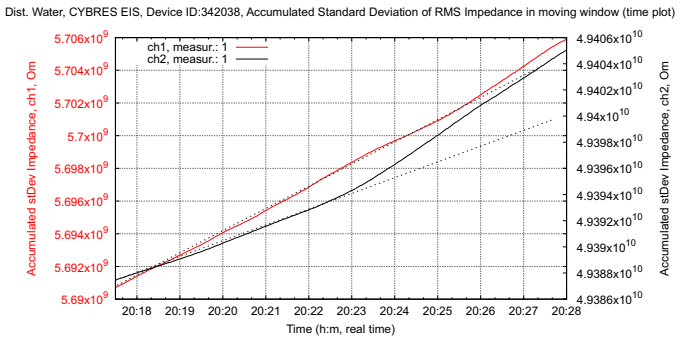

(b)

Fig. 9. **(a)** Example of $Var(M^{RMS}(t))$ (variation of RMS impedance calculated in the moving window) and **(b)** $V(t) = \sum Var(t)$ (accumulated values of $Var(M^{RMS}(t))$), the moving window is of 70 values (70 sec.) for the data from Fig. 1(b).

some specific time interval between t_1 and t_2):

$$\Delta V = V(t_2) - V(t_1), \tag{31}$$
$$\Delta S = S(t_2) - S(t_1), \tag{32}$$
$$\Delta K = K(t_2) - K(t_1). \tag{33}$$

ΔV has the same dimension as $M^{RMS}(t)$, $P^C(t)$ and $C(t)$, however ΔS and ΔK are dimensionless and vary around zero, i.e. their accumulation has a non-increasing character and thus differs from ΔV. To have a similar dynamical behaviour for all ΔV, the coefficients k_s and k_k in (25) and (26) are selected so that to keep an increasing dynamics of all ΔV ($k_s = 3$ and $k_k = 3$).

All Δ are sensitive to the dynamics of $\overline{\Phi(t)}$ and are calculated for the first and the second channel as $\Delta^{1,2}$. Following the concept of differential measurements, we define a relationship between channels as

$$dV = \frac{\Delta^1 V}{\Delta^2 V}, dS = \frac{\Delta^1 S}{\Delta^2 S}, dK = \frac{\Delta^1 K}{\Delta^2 K}, \tag{34}$$

$$\overline{d\Phi(t)} = \begin{bmatrix} dV(M^{RMS}) \\ dV(P^C) \\ dV(C) \\ dS(M^{RMS}) \\ dS(P^C) \\ dS(C) \\ dK(M^{RMS}) \\ dK(P^C) \\ dK(C) \end{bmatrix}. \tag{35}$$

The values of $\overline{d\Phi(t)}$ are understood as a statistical relationship between control and experimental samples, where 0% – means both samples are statistically equal. Parameters dV, dS and dK calculated for $M^{RMS}(t)$, $P^C(t)$ and $C(t)$ allow characterizing different aspects of this relationship. **The parameter 'Total Score' calculated as averaging of dV, dS and dK, can be considered as a single-value parameter that characterizes the experimental sample against the control.** This approach is implemented as a two-pass algorithm [11, p.613].

The values of $\overline{d\Phi(t)}$, calculated in %, are plotted as

$$\begin{aligned} if(\Delta^1 > \Delta^2) \quad &\longrightarrow \quad -(1 - \overline{d\Phi(t)}) * 100 \\ if(\Delta^1 > \Delta^2) \quad &\longrightarrow \quad (1 - \overline{d\Phi(t)^{-1}}) * 100 \end{aligned} \tag{36}$$

with bar charts for 2,3 and 4 moments. The expression (36) allows obtaining additional information about inhibition/stimulation behaviour of corresponding channel. Note that that bars go up and down in the diagram, however the absolute values are displayed; the 'Total Score' is calculated based on absolute values, see Fig.13.

VII. Measurements of noise

As mentioned, electrochemical noise has two components: short-term fluctuations of current and potential, and a middle-term and long-term variation of electrochemical stability. Both components represent different properties and are measured in different way.

Signal scope measurement of short-term noise. The primary source of noise is the signal scope measurement, which samples the excitation $V_V^f(n)$ and response $V_I^f(n)$ signals, see Fig. 3. The parameter n is a number of samples, typically the EIS system at each single run samples about 8400 values for two channels of $V_V^f(n)$ and $V_I^f(n)$.

Due to analog circuitry of the EIS system, the noise on electrodes (applied to water) and sampled via ADC are different in regard to high frequency components. Sampling the response signal with disconnected electrodes (with settings that maximize the EIS noise), we receive the EIS noise with the amplitude of low frequency components about 2-3mV and amplitude of high frequency components $<$ 0.5mV, see Fig. 11.

The short-term noise represents a combination of EIS noise and a response of the test object to the excitation signal that contains the EIS noise. The noise-to-signal ratio depends on the excitation voltage: on the high excitation voltage range $\pm 1V$ it is about 400, on the low excitation voltage range $\pm 100mV$ it is about 20. Another issue that needs to take into account is the distortion of excitation signal due to a digital signal synthesis. This can be considered similar to white-noise excitation for fast EIS [6] and generally contributes to the noise generation in water.

Thus, the short-term noise is available in the signal scope mode, and it is sensitive to the sampling frequency of ADC, and the excitation voltage range. Sinusoidal form of excitation signal represents one of difficulties for statistical calculation (22)-(35). Since the integrals $V(t)$, $S(t)$ and $K(t)$ as well as ΔV, ΔS and ΔK require only positive values to generate an increasing dynamics (that underlies the proper calculation of dV, dS and dK), we apply a linear shift of $V_I^{f,t}$

$$\tilde{V}_I^{f,t} = V_I^{f,t} + \tilde{k}. \tag{37}$$

The value of $\tilde{k}$ is selected so that all components of $V_I^{f,t}$ are positive. Since $\tilde{k}$ is incorporated into the numerator and denominator of (34), it does not essentially affect the calculations. However, it needs to take into account that large values of $\tilde{k}$ decrease the sensitivity (since the signal becomes much larger than the noise), small values of $\tilde{k}$ decrease the reproducibility of results (since the noise has a larger contribution in the common dynamics). Thus, $\tilde{k}$ represents a compromise between sensitivity and reproducibility of statistical measurements in the signal scope mode. Based on performed tests it is recommended to perform measurements on the middle range of excitation signal, it provides enough sensitivity as well as good reproducibility, see Fig. 10. Measurements on the lowest range of excitation signal contain a high random dynamics and therefore are not recommended.

Continuous measurements with constant f of long-term electrochemical stability. The signal scope mode handles the short-term noise dynamics, however is not able to measure a middle-term and a long-term variation of electrochemical stability. Due to variation of stability, multiple iterative fluidic measurements in the signal scope can produce changing values. For representation of middle-term and a long-term dynamics, it needs to switch to continuous measurements with constant f.

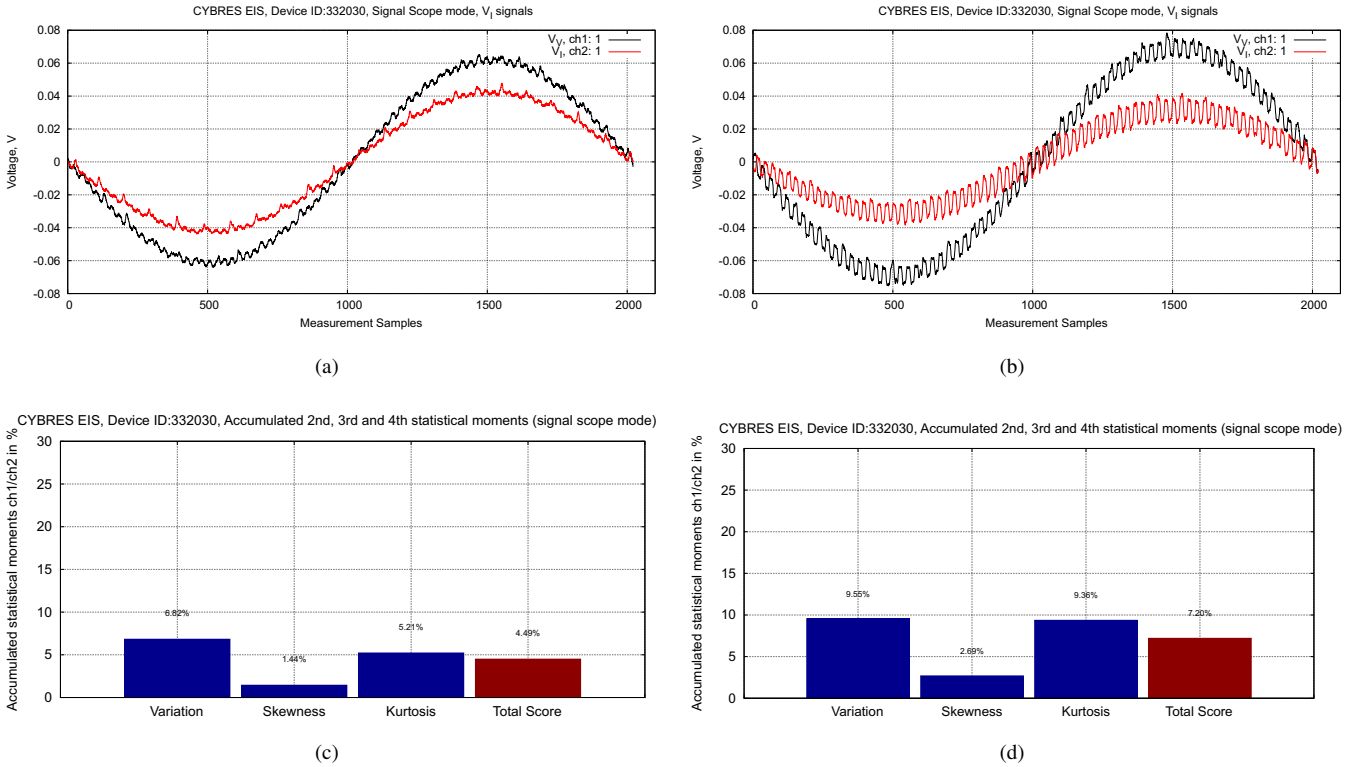

Fig. 10. Two examples of statistical measurement in the signal scope mode. **(a,b)** Response signals from two different pairs of water samples (both are non-chemically treated in different ways); **(c,d)** Bar charts to the corresponding signals; amplification 50000, middle signal range.

Secondly, the values of $M^{RMS}(f)$, $C(f)$ and $P^C(f)$ are sensitive to the variation of means, calculated by (22) in a moving window, and thus, to the electrochemical stability.

Middle- and long-term variations of electrochemical stability reflect changes on the ionic level caused by different factors. Beside gas dissolving and self-ionization processes, the electrochemical stability represents a reaction on the excitation voltage (as mentioned, the EIS is an example of excitation spectroscopy). Degradation of impedance is well observable on the high level of excitation voltage and is almost not present of the lowest level – this can underlay corresponding measurement

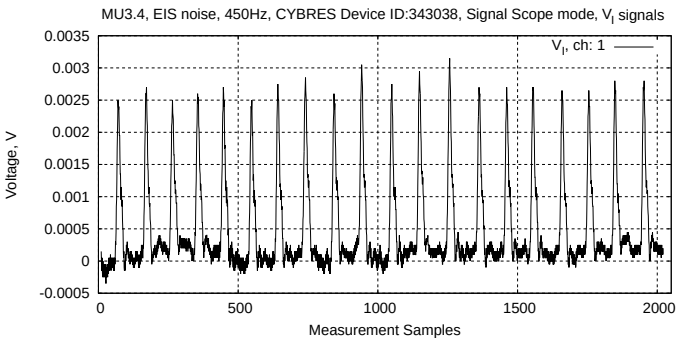

Fig. 11. Worst case of the EIS noise measured as the response signal with disconnected electrodes on the output of amplifier with maximal amplification factor 50000 (DAC, ADC, analog and digital multiplexers are on, maximal clock frequency). The EIS noise does not represent the system's noise.

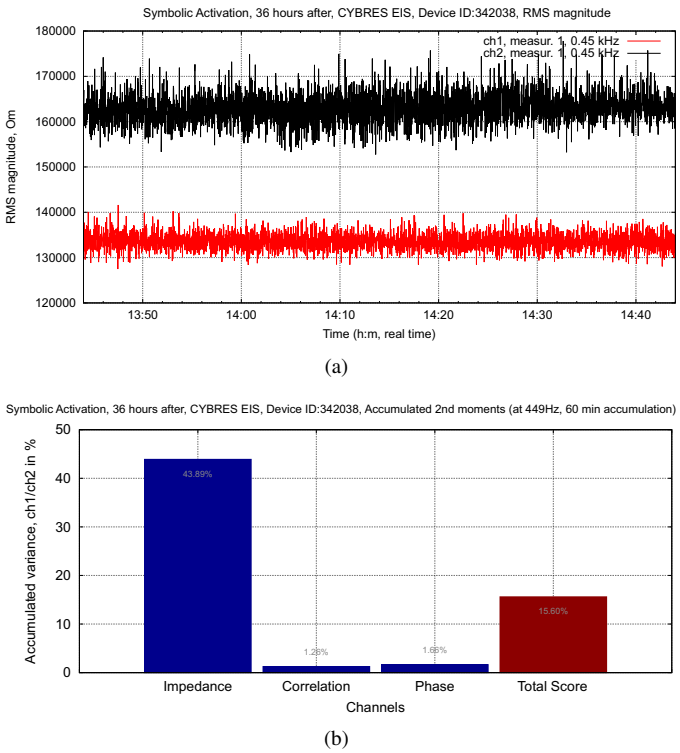

Fig. 12. Continuous measurements with constant f, shown are the second statistical moments. **(a)** The signals have stable temporal dynamics but different impedance with different noise level that reflects also in **(b)** variation of noise.

strategies.

Since electrochemical stability depends on many factors such as the used electrodes and fluids, the measurement time and experimental conditions, the results of measurements in this mode can vary between different setups. In order to make measurements invariant to setups, it needs to use the time-differential strategy as described in [3]. It requires to define two regions of measurements: the region of background measurement $\overline{d\Phi(t_b)}$ and the region of experimental measurement $\overline{d\Phi(t_e)}$. The final result represents a subtraction of both regions

$$\overline{d\Phi(t_b)} - \overline{d\Phi(t_e)} \tag{38}$$

The background region can be subtracted from experimental one, or vice versa, the experimental region can be subtracted from background one. This feature is used for online/offline statistical calculations, see Sec. XI. It is recommended to use the expression (38), since it increases repeatability of results in the continuous measurements mode.

Note that the sign of (36) and (38) can represent a source of additional information, about inhibition/stimulation behaviour of corresponding channel, see Fig.13.

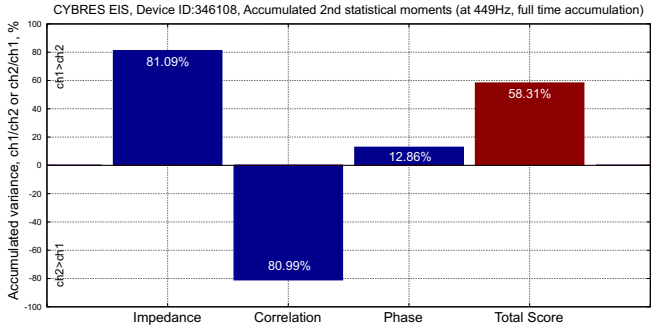

(a)

Fig. 13. Bar diagram calculated with sign of (36) and (38).

VIII. Implementation

This analysis is implemented in the DA module and run as a post processing of measured data. If the MU device is connected and configured as EIS, the client recognizes this and calls the script 'init/configureDA_EIS.ini' (for continuous measurements) or 'init/configureDA_EIS_sig.ini' (for signal scope mode). Biosensor uses the script 'init/configureDA_bio.ini' and phytosensor 'init/configureDA_phy.ini' These scripts are not executed when the already recorded and processed data are read from file. This call is executed independently of custom initialization of DA (e.g. if 'usingActuators=0', the script 'init/configureDA_EIS.ini' will be still executed). The DA module has specific numerical processors 241 (for continuous mode)

```
-- enable statistical processor for EIS
bufferSizeDataPipes=500;
I241=1;
```

and 242 (for signal scope)

```
-- enable stat. processor for signal scope
bufferSizeDataPipes=500;
I242=1;
```

that perform all necessary calculations. Note that statistical calculation are sensitive to the buffer size defined by the parameter 'bufferSizeDataPipes', use always the same buffer size for calculation that should be compared with each other. Overview of numerical processors from DA module used in post-processing of statistical data is shown in Table II.

TABLE II
Numerical processors of DA module used in post-processing of statistical data.

N of num. proc.	position in data file	description
241	34-51	it calculates 2nd–4th order statistics for Impedance, Correlation and Phase (continuous mode)
242	11-16	it calculates statist. data for the EIS signal scope mode (2nd–4th order statistics for raw signals)
243	34-59	it calculates 2nd–4th order statistics for Impedance, Correlation, Phase and Temperature (continuous mode)
244	34-59	the same as 243 but for temperature data accumulated in MU32 systems
245	34-59	it **re-calculates** 2nd–4th order statistics for Impedance, Correlation, Phase and Temperature **read from file, positions 1-33** and write them into _ND.dat file (positions 34-59)
246	34-51	it **re-calculates** 2nd–4th order statistics for Impedance, Correlation and Phase **read from file, positions 1-33** and write them into _ND.dat file (positions 34-51)

Possible collisions between DA_EIS and custom DA scripts. The DA_EIS script uses the positions after 34 (processors 242, 243, 246 use positions 34-51, processors 243–245 use positions 34–59) of the main data file (positions 1-33 represent data from the MU device). Thus, all custom DA scripts should use the positions after the 51 (or 59). Since the DA module allows using of only 70 data channels, users should take care of keeping the maximal value 70 for EIS/biosensor applications. The variables 'bufferSizeDataPipes' define the size of input data buffers (used for calculations of running means in corresponding modes). The value 'bufferSizeDataPipes' defined in different scripts are handled as 'last used', i.e. last defined script defined the value of 'bufferSizeDataPipes' for all DA scripts.

Signal scope mode with statistically significant number of measurement. This option implements the signal scope measurement that provides statistically significant number of iterations. Select in plot 'signal scope' and in channels 'bar chart 30 iter', see Fig 14.

After this press the 'Measurements start'. Note that this measurement has different data format for the '_sig' file and thus requires starting the new measurements! The EIS system will perform 30 independent measurements, the bar charts show the mean values for variation, skewness, kurtosis and total score from these 30 measurements (all 30 measurements are available in the file '_sig'). To suppress the sound indication of iterative starts, press the 'sound off'. To turn on the sound indication, press the 'sound on'.

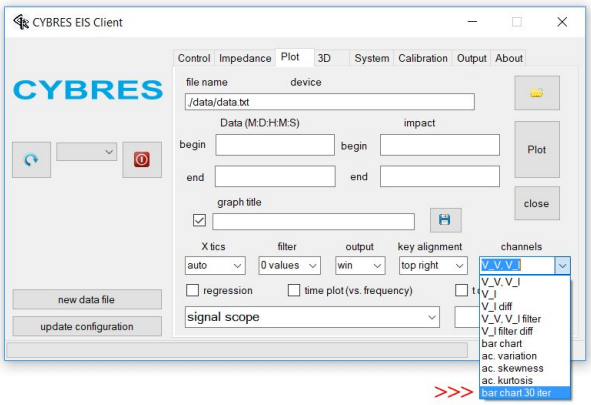

(a)

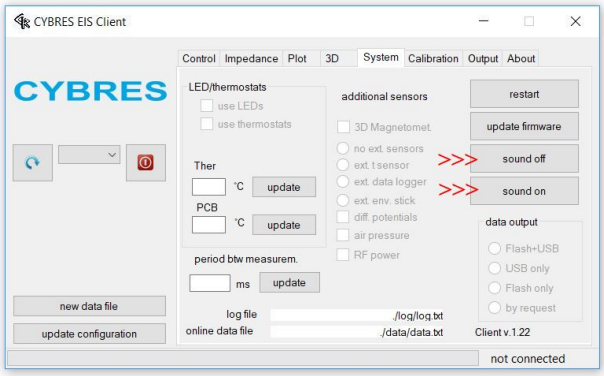

(b)

Fig. 14. **(a)** Selection the signal scope mode with statistically significant number of measurement; **(b)** Suppressing the sound indication of EIS.

TABLE III
CALIBRATION ATTEMPTS, SHOWN ARE THE 'TOTAL SCORE' FROM 'BAR CHART 30 ITER' MODE (900 AVERAGED WITHIN 30 MEASUREMENTS, IN TOTAL 5400 MEASUREMENTS), 'R/200' MEANS – USING TWO 52KOM RESISTORS WITH $\tilde{k} = 200$, 'W2/300' – WATER, SAMPLES N2, $\tilde{k} = 300$.

N	R/200	R/300	W1/200	W1/300	W2/200	W2/300
1	0.211	0.203	1.016	0.642	10.292	5.445
2	0.230	0.179	0.968	0.738	10.156	5.311
3	0.197	0.206	1.052	0.668	10.175	5.398
4	0.190	0.212	1.065	0.773	10.138	5.52
5	0.207	0.190	1.045	0.608	10.241	5.435
6	0.241	0.205	1.016	0.653	10.185	5.343
7	0.181	0.205	1.006	0.664	10.267	5.341
8	0.230	0.194	1.033	0.7	10.352	5.37
9	0.191	0.169	1.094	0.742	10.326	5.328
10	0.192	0.197	1.08	0.818	10.237	5.472
11	0.224	0.192	0.973	0.711	10.31	5.452
12	0.169	0.223	1.146	0.644	10.391	5.422
13	0.205	0.199	1.023	0.716	10.413	5.48
14	0.208	0.191	1.021	0.744	10.472	5.466
15	0.182	0.197	0.975	0.674	10.444	5.458
16	0.218	0.193	1.011	0.692	10.417	5.461
17	0.222	0.209	0.958	0.709	10.301	5.412
18	0.207	0.171	1.015	0.728	10.405	5.496
19	0.209	0.206	1.046	0.681	10.344	5.583
20	0.189	0.187	0.953	0.647	10.37	5.529
21	0.186	0.196	1.005	0.712	10.427	5.624
22	0.219	0.209	1.006	0.694	10.441	5.532
23	0.175	0.165	0.968	0.76	10.542	5.554
24	0.217	0.178	1.045	0.74	10.494	5.491
25	0.212	0.182	1.039	0.709	10.507	5.448
26	0.197	0.198	1.051	0.72	10.581	5.463
27	0.222	0.217	1.001	0.645	10.517	5.481
28	0.198	0.180	1.066	0.672	10.549	5.515
29	0.198	0.202	1.013	0.76	10.54	5.595
30	0.200	0.175	1.062	0.721	10.745	5.529
μ	0.204	0.194	1.025	0.702	10.385	5.465
σ	0.017	0.014	0.042	0.045	0.139	0.076

IX. CALIBRATION

Signal scope mode. Tests and calibration have been performed in the signal scope mode with 1) two resistors 52kOm inserted into thermostabilized container, see Fig. 16; 2) unprocessed distilled water (denoted as W1); 3) non-chemically treated distilled water (denoted as W2). All measurements are performed in thermally stable environment, PCB thermostat is on. We measured twice for each of 1)-3) with $\tilde{k} = 200$ and $\tilde{k} = 300$ to estimate the impact of (37) on statistical analysis in the scope mode.

Table III shows the results for external resistors and different water for $\tilde{k} = 200$ and $\tilde{k} = 300$ (the middle excitation signal range). These attempts utilize the approach '30 iteration' (each single value is calculated based on 30 independent measurements, 900 measurements for one category, in total 5400 measurements, each new measurement is performed after 5 sec. interval). As expected, $\tilde{k} = 300$ provides smaller variation and smaller 'total score' values. For W2/200 and W2/300 we observe an essential difference between $\tilde{k} = 300$ and $\tilde{k} = 200$.

Table IV demonstrates these results without intermediate averaging – μ and σ are calculated directly from 900 measurements in each category. As expected we observe larger μ and σ, which however are accounted only for 'variation'. Parameters 'skewness' and 'kurtosis' remain stable in respect to variation of $\tilde{k}$ and averaging strategy (we will return to this point later). Thus, 30 iteration for a single value (implemented as 'bar char 30 iter') provide higher accuracy of measurements.

Another expected result – the larger is the value μ, the smaller is the deviation σ (in %), e.g. 8.4% in R200 up to 1.3% in W2/200. This is well-known fact in metrology (measurement error on the end of scale [12], [13]) and allows estimating accuracy of 'total score' about 10% for readings on the scale $> 0.1\%$, 5% for readings on the scale $> 1\%$ and about 1% for readings on the scale $> 10\%$. Since non-chemical water treatments are usually performed on the $> 10\%$ scales of 'total score', we can expect about 1% accuracy of this method in the signal scope mode on the middle average excitation range (± 0.1V). Thus, $\tilde{k} = 200$ provides better strategy (i.e. only shift to achieve positive values of $V_I^{f,t}$) in achieving higher relative accuracy.

Another issue, which became remarkable – repeating 900 measurements during 90 min did not demonstrate a degradation of values at the middle range of excitation signal, see Table III. Thus, 30 iterative measurements on this excitation range can be considered as not disturbing the electrochemical stability.

Continuous mode. Calibration measurements in the contin-

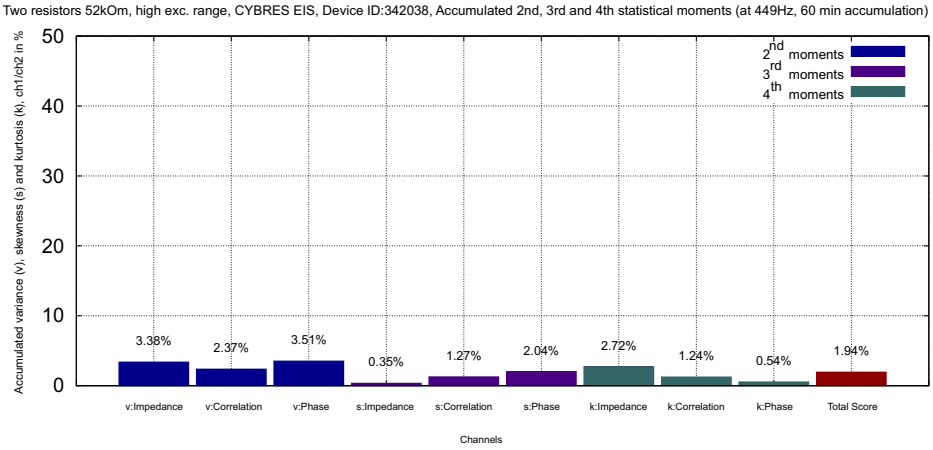

(a)

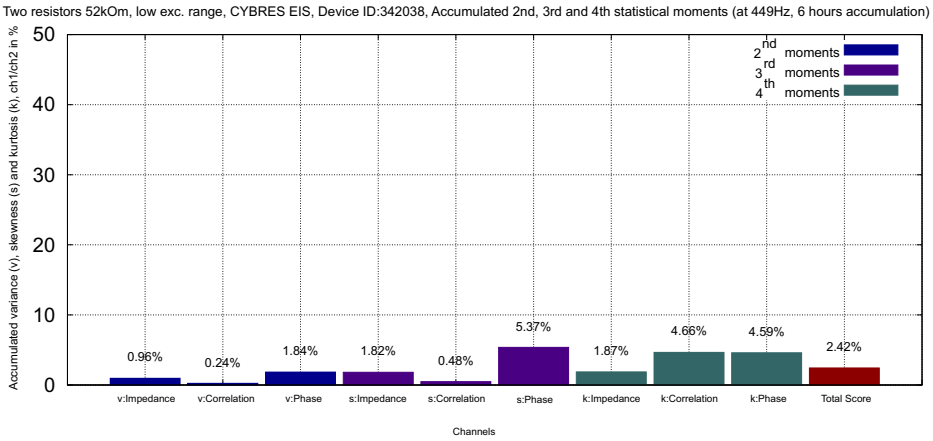

(b)

Fig. 15. Example of bar charts for 2,3 and 4 moments calculated based on (31) as relation between ch1 and ch2 (in %) of accumulated moments. Shown is the test measurement with two external resistors 52kOm: **(a)** the high range of excitation signal, accumulation time 60 minutes; **(b)** the low range of excitation signal, accumulation time 6 hours.

Fig. 16. Setup with two resistors on 52kOm inserted into thermostabilized container.

uous mode with external resistors are shown in Fig. 15. Tested are the high and the low excitation ranges – the high excitation range generates more intensive electrochemical variations, whereas the lowest excitation range involves physical noise into calculations. This measurement does not involve the approach (38) since resistors do not demonstrate degradation of parameters. Measurements in this mode require a long sampling time, it is recommended to use 60 min and 180 min accumulation time.

Using the continuous mode with fluids (in the middle and high range of excitation signal) in fact tests dynamical properties of electrochemical system and generally depends on the selected region of dynamics (see discussions in the next section). To test the approach (38), we used multiple EIS devices working in parallel during several days. Thereby different electrodes and different freshly-filled and long-time-used distilled water was used. To minimize any natural and artificial impact on water during measurements, the background region was selected in the time from 0:00 up to 2:00 and the experimental region – from 2:00 up to 4:00 (each night). All samples during

TABLE IV
CALIBRATION ATTEMPTS, μ (MEAN) AND σ (STANDARD DEVIATION) ARE CALCULATED FROM 900 SAMPLES FOR EACH ATTEMPT IN EACH CATEGORY (R/200,300, W1,2/200,300) WITHOUT INTERMEDIATE AVERAGING (IN TOTAL 5400 MEASUREMENTS); SHOWN ARE THE 'VARIATION, 'SKEWNESS', 'KURTOSIS', AND 'TOTAL SCORE' AS REPRESENTED IN BAR CHARTS.

	variation	skewness	kurtosis	total score
R/200				
μ	0.146	0.161	0.306	0.204
σ	0.113	0.123	0.238	0.103
R/300				
μ	0.125	0.157	0.300	0.194
σ	0.095	0.120	0.229	0.094
W1/200				
μ	1.922	0.470	0.683	1.025
σ	0.430	0.350	0.540	0.256
W1/300				
μ	1.004	0.471	0.633	0.703
σ	0.310	0.361	0.494	0.240
W2/200				
μ	22.370	1.437	7.351	10.386
σ	0.768	0.530	1.006	0.339
W2/300				
μ	7.479	0.767	8.149	5.465
σ	0.432	0.438	0.876	0.283

measurements are stored in styrofoam boxes as shown in Fig. 17. We noted that initial EIS dynamics after filling containers

TABLE V
CALIBRATION ATTEMPTS (CONTINUOUS MODE), THE TIME DIFFERENTIAL APPROACH (38) IS USED, THE BACKGROUND MEASUREMENT – FROM 0:00 UP TO 2:00, THE EXPERIMENTAL MEASUREMENT – FROM 2:00 UP TO 4:00, RESULTS OF 'TOTAL SCORE' FOR EIS DEVICES ARE SHOWN.

N	EIS1	EIS2	EIS3	EIS4	EIS5
3.9	3.66	4.27	3.87	1.74	5.56
2.9	8.08	2.04	3.92	6.42	3.42
1.9	8.86	4.53	4.19	2.77	4.21
31.8	—	—	7.77	—	—

with water demonstrates a high level of instability reflecting in 6%-8% of 'total score'. The same water but after a resting period demonstrates about 2%-5% of 'total score'. Minimal perturbations (for instance 'morning perturbations' that occur each morning) are on the level of 12%-15% and more.

X. MEASUREMENT STRATEGY

Before using statistical module (or any other mode of EIS device), it needs to answer two following questions that define the measurement strategy.

1. Should I perform a non-chemical treatment before or during measurement?

Specific weak impact factors require sometimes a long exposure of fluids. Non-chemical treatment of samples before measurements provides more time for manifestation of ionic changes and thus makes it more 'visible' for measurements. However, during this time the fluids become exposed by environmental factors (e.g. light, EM and electrostatic fields, CO2 from air, etc.), so that it is difficult to recognize whether

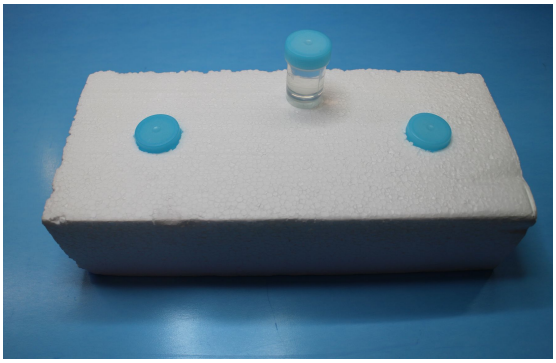

Fig. 17. Temporary storage of water containers in styrofoam box, it protects samples from thermal and light impact, the box can be wrapped into the aluminium foil for shielding (to some extent) against electromagnetic and electrostatic fields. The box (samples) should not be mechanically distorted (vibrations or shaking).

electrochemical changes are caused by non-chemical treatment or by environmental factors. If a long exposure is required, make sure that control and experimental samples are stored in the same conditions and try to minimize environmental influences, see e.g. Fig. 17. In some cases, samples should be exposed to environmental influences (e.g. sun light), here it is important to design experiments in such a way so that control and experimental samples differ only in one impact factor.

Measurements during non-chemical treatment is more accurate because it minimizes impact of environmental factors. Moreover, two parts of continuous measurement (the background recording and experimental part) enable identifying the causal dependency between non-chemical treatment and electrochemical changes. Whenever it is possible, the non-chemical treatment during measurements (in continuous mode) is more preferable.

2. Should I test statical or dynamical properties of fluids?

Test of statical properties means one-time measurement (e.g. spectrogram, conductivity value, statistical properties of noise in signal scope, pH etc.) with a minimal excitation of fluids. It is well suitable if a non-chemical treatment provides essential electrochemical changes. Advantage of statical tests is the stability and reproducibility of measurements.

In case of weak changes, statical properties do not provide enough information, and it needs to test dynamical properties. In this case the fluid is excited by temperature, electric current, light or EM fields and the EIS system measures a response. As already mentioned, EIS itself is an example of excitation spectroscopy. General observation is that non-chemically treated fluids demonstrate more 'active' dynamics. It includes variation of potential, spikes, appearance of oscillations and other effects that are not characteristic for unprocessed fluids. Such effects are detectable by statistical module, see Fig. 18. The disadvantage of excitation approach consists in non-linearity that reflects in reducing reproducibility.

It is recommended to start with the test of statical properties – for EIS it means a small measurement time, using signal scope mode for statistical analysis, selection of middle and small ranges of the excitation signal. When this mode does not provide enough information (there are no differences between

control and experimental fluids), apply tests on dynamical properties. For EIS it means using a long measurement time, performing statistical analysis in continuous mode, selection of a maximal range of the excitation signal.

XI. How to perform measurements with the statistical module

To start measurements in this mode it needs to remove all low pass filters and to select the excitation range that corresponds to the used measurement strategy, see Fig. 19. The hardware device should be configured as EIS (for reconfigurable MU devices with changeable electrodes for phyto-/bio- and EIS measurements).

1. **Selection of frequency.** Both ADCs work in 1.1 Msps mode in the frequency range from 450Hz, it is recommended to use this frequency for statistical measurements in signal scope mode. Note that a low frequency leads to the polarization of electrodes, see e.g. [14], and potentially produce larger statistical results in the continuous mode (however the polarized electrodes can additionally increase a sensitive of EIS sensors). General recommendation is to test several frequencies from very low up to 3-5kHz for measurements in the continuous mode.

2. **Selecting the range of the excitation signal.** This selection depends on the selected strategy of measurements, see Sec. X. Testing statical properties is more suitable in lower and middle excitation ranges, tests of dynamical properties requires a high excitation voltage. Test always the right selection for the range of excitation signal as well as settings for the amplitude in the signal scope mode (it should correspond to the conductivity of the used fluid). **Make sure that sinusoidal signals are not distorted in the signal scope**, otherwise EIS measurements are not valid.

3. **DDS type.** Use 'signal scope' and 'continuous measurement (fixed f)' for statistical module. Other measurement modes do not support the statistical analysis.

4. **Remove all low pass filters.** Set 0 in 'input LP filter', 'output LP filter' and set 1 in the field 'aver. filter', see Fig. 19. Press 'update parameters'.

5. **Measurements in the signal scope mode.** Results are available in the 'signal scope', see Fig.14. It is recommended to use a statistically significant number of iterations as described in Sec. VIII.

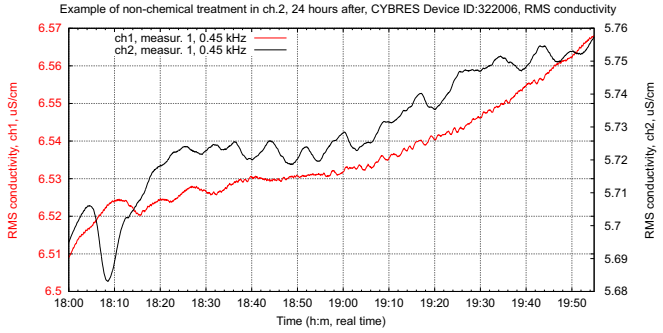

(a)

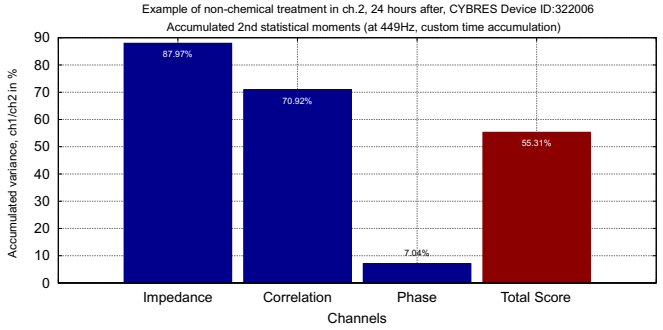

(b)

Fig. 18. **(a)** Tests of dynamical properties – example of unstable electrochemical dynamics of a fluid that was non-chemically treated (the channel 2, high range of excitation signal); **(b)** Statistical measurements of (a) in the continuous mode that reflect the difference between channels (processed and unprocessed fluids).

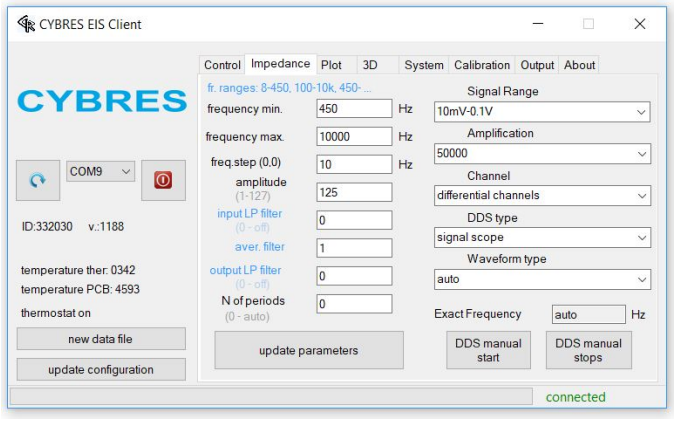

Fig. 19. Settings for measurements with statistical module.

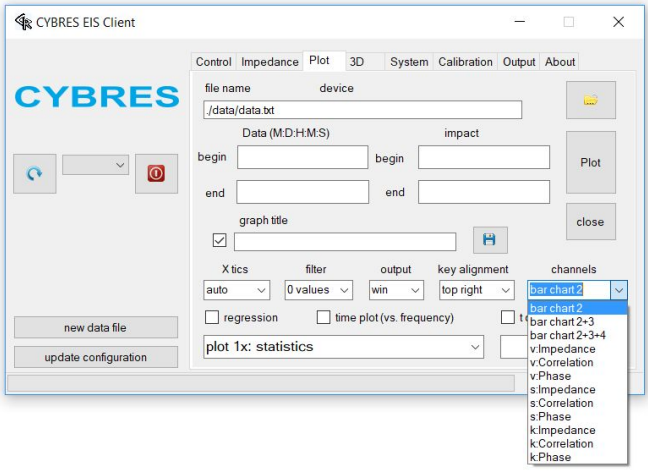

Fig. 20. Available plots for 'continuous measurement (fixed f)'.

6. **Measurements in the continuous mode.** Results of measurements in this mode are available in the 'plot 1x:statistics', see Fig. 22. It is strongly recommended to utilize the time-differential approach with background/experimental time-regions, expressed by (38). First, perform the background

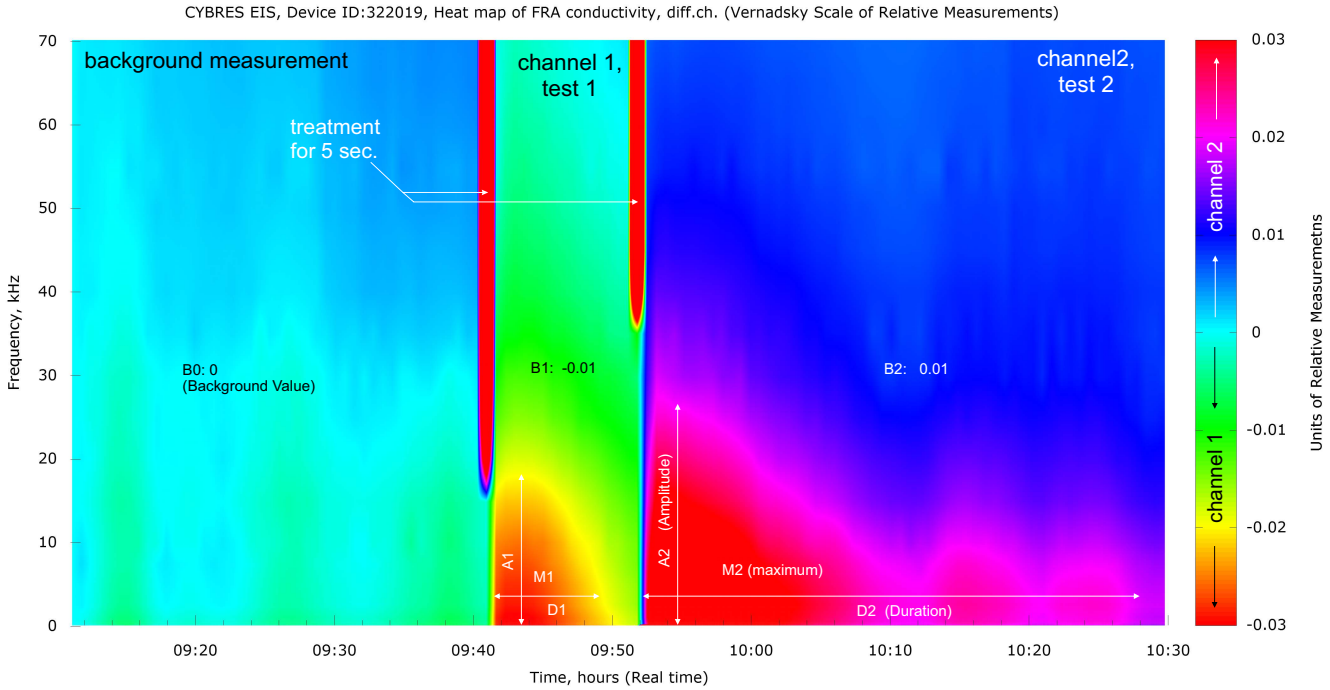

Fig. 21. EIS measurement with TdM (treatment-during-measurement) strategy of non-chemical treatment for 5 sec. (continuous measurement, shown is the differential channel).

measurement, when fluids are undistorted. This represents a reference point for statistical calculation. Enter time of this region into the fields 'impact begin' and 'impact end', as shown in Fig. 22. Then, apply experimental factors to fluids (without removing electrodes from containers, containers should remain mechanically undistorted) – this represents the experimental measurement. Write the 'begin time' of experimental measurement in the fields 'begin'. During online measurements, the field 'end' is changing automatically, representing always the last sampled value from EIS device. Thus, during online measurements only the last region can represent the experimental region. For offline plots (reading data from file), the experimental and background regions can be selected arbitrarily, for instance the experimental time can be inserted in the fields 'impact'.

Note that background and experimental measurements should be equally long – this allows removing the systematic instability in the most optimal way. These regions should not cover each other, otherwise this will reduce the reproducibility of measurements. For offline plots, different parts of EIS dynamics (even with long pause between each other) can be used as background and experimental regions. This allows analysing the long-term measurements (in term of days or weeks).

Simple biophysical tests. Simple tests of statistical module can be performed by holding one of containers with water in hand for several seconds (with minimal mechanical distortions). Use for this the EIS device with open electrodes, which have built-in temperature sensors inside the fluids.

After putting the water container back to the holder, leave enough time for equalizing the temperature in containers. For example, 5 sec. keep-in-hand time requires about 20-30 minutes

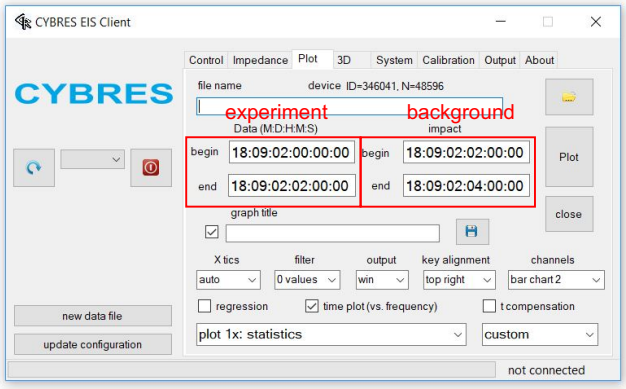

Fig. 22. Setting of experimental and background regions. Note, that for online measurements the background region should be inserted in the fields 'impact' and only the last region can represent the experiment. For offline plots (reading data from file), the experimental and background regions can be selected arbitrarily, for instance the experimental time can be inserted in the fields 'impact'.

of resting. Perform temperature measurements before and after handling, the temperature difference between containers is typically < 0.01C, see Fig. 23. The statistical measurement after handling is valid if the temperature difference between containers remains on a similar level as before handling. Especially interesting results appear after multiple handling, e.g. during several days.

This measurement can be performed in the signal scope mode (two times – before and after handling). Another strategy is to continuously measure during the handling (in continuous

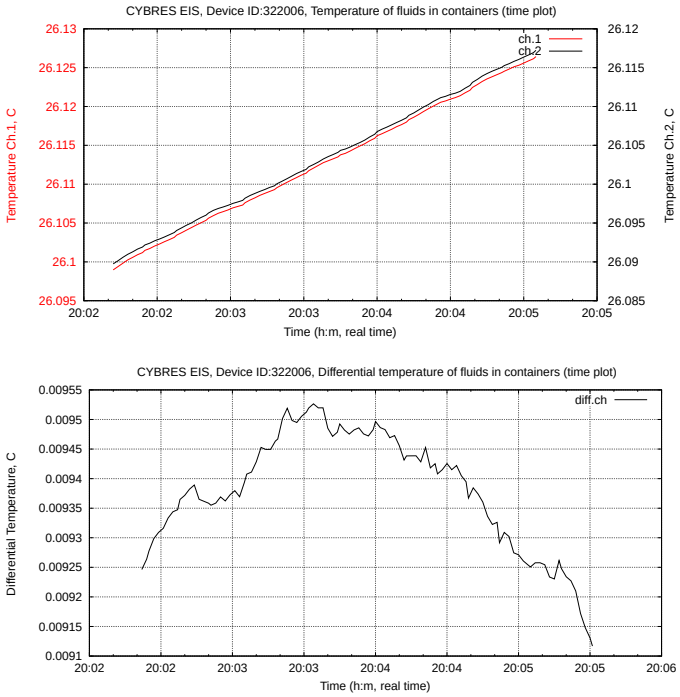

Fig. 23. Temperature measurements inside the fluids, typical temperature difference between containers is < 0.01C.

mode with fixed f) – all electrochemical processes before, during and after handling will be well visible, see Fig. 21. Here, first the channel 1 is handled, after this, in 10-20 minutes – the channel 2. This strategy allows reducing the measurement time since both channels are affected by temperature in the same way. These approaches can underlie some dedicated biophysical measurements.

XII. Conclusion

This application note provided theoretical explanations as well as practical recommendations for using the statistical and spectral modules of EIS device. These descriptions are useful as a one-number or vector characteristics of non-chemical treatment. The statistical/spectral approaches are implemented in two different modes and allow characterizing a non-chemical treatment in fast and well reproducible way. Calibration and different measurement strategies for non-chemical treatment are discussed and illustrated by examples.

XIII. Disclaimer

This application note means an open-science approach of experimental nature. When using this approach and corresponding implementations in CYBRES MU devices – considered as a service from CYBRES GmbH – its experimental character in relation to methodology, equipment or accuracy should be always considered. Remember, a single measurement has a probabilistic nature. Before drawing any conclusions, a statistically significant number of independent attempts (> 30) should be undertaken. CYBRES GmbH does not assume any liability arising out of the application or use of any part of this service, and specifically disclaims any and all liability, including without limitation special, consequential or incidental damages of any kind. CYBRES GmbH can any time change this service, add/remove diverse functionality. CYBRES GmbH follows the data protection rules, any requests/data exchange remain confidential as long as other agreements with corresponding partners are not achieved. Graphical images are allowed to copy when the word 'Cybertronica Research' or 'CYBRES' remains on caption to these images. Any citations or references on graphical/technical material should include links to CYBRES GmbH.

References

[1] CYBRES, Differential Impedance Spectrometer for electrochemical and electrophysiological analysis of fluids and organic tissues. Handbook and User Manual, CYBRES GmbH, 2024.
URL https://cybertronica.co/download/MU-EIS_Manual_en.pdf

[2] S. Kernbach, I. Kuksin, O. Kernbach, On accurate differential measurements with electrochemical impedance spectroscopy, WATER 8 (2017) 136–155. doi:10.14294/WATER.2016.8.

[3] S. Kernbach, Application Note 20. Increasing accuracy of repeated EIS measurements, CYBRES, 2017.

[4] S. Kernbach, I. Kuksin, O. Kernbach, A. Kernbach, On metrology of electrochemical impedance spectroscopy in time-frequency domain, IJUS 143–150 (5) (2017) 62–87. doi:10.17613/zh5b-jd94.

[5] P. L. Geissler, C. Dellago, D. Chandler, J. Hutter, M. Parrinello, Autoionization in Liquid Water, Science 291 (2001) 2121–2124. doi:10.1126/science.1056991.

[6] P. Boškoski, A. Debenjak, B. Boshkoska, Fast Electrochemical Impedance Spectroscopy: As a Statistical Condition Monitoring Tool, Springer Briefs in Applied Sciences and Technology, Springer International Publishing, 2017.

[7] R. A. Cottis, Interpretation of electrochemical noise data, CORROSION 57 (3) (2001) 265–285. doi:10.5006/1.3290350.

[8] C. Loto, Electrochemical noise measurement technique in corrosion research, Int. J. Electrochem. Sci. 7 (2012) 9248–9270.

[9] S. Kernbach, Application Note 26. Methodology and protocols of feedback-based EIS experiments in real time, CYBRES, 2019.
URL www.cybertronica.de.com/download/CYBRES_Application_Note_26.pdf

[10] S. Kernbach, Application Note 27. Using regression scan for electrochemical 'treatment-during-measurement' experiments, 2020. doi:10.13140/RG.2.2.24161.93280.
URL http://cybertronica.de.com/download/CYBRES_Application_Note_27.pdf

[11] W. H. Press, S. A. Teukolsky, W. T. Vetterling, B. P. Flannery, Numerical Recipes in C (2Nd Ed.): The Art of Scientific Computing, Cambridge University Press, New York, NY, USA, 1992.

[12] T. Rathore, Digital Measurement Techniques, Alpha Science, 2003.
URL https://books.google.de/books?id=5UuRiXkfYlwC

[13] H. Czichos, T. Saito, L. Smith, Springer Handbook of Metrology and Testing, Springer Handbooks, Springer Berlin Heidelberg, 2011.
URL https://books.google.de/books?id=fpTE1Z5UfsQC

[14] S. Kernbach, Replication attempt: Measuring water conductivity with polarized electrodes, Journal of Scientific Exploration 27 (1) (2013) 69–105.